Improving Convergence Rates in Simulated Annealing trough Funnel Search Neighborhoods: an application to Heterogeneous Multistatic Sonar Network Configuration

Owein THUILLIER[a,b], Nicolas LE JOSSE[a], Alexandru-Liviu OLTEANU[b], Marc SEVAUX[b], Hervé Tanguy[a]

[a]Thales, Defence and Mission Systems (DMS), Brest, France
firstname.lastname@fr.thalesgroup.com
[b]Université Bretagne-Sud (UBS), Lab-STICC, UMR CNRS 6285, Lorient, France
firstname.lastname@univ-ubs.fr

1 Introduction

In the context of Anti-Submarine Warfare (ASW), sonar systems have been used for decades as an effective means of probing the oceans, whether it is to search, locate or track underwater threats. Therefore, decision support on these different systems is an important axis for ASW decision-makers and it is in this perspective that this work is articulated.

First and foremost, two main types of sonar systems co-exist. On one hand, there are passive sonar systems that listen to the sounds radiated by underwater sources, and, on the other hand, there are active sonar systems that emit a sound pulse and receive the reflected wave (echo) on the target [1]. It is this last category which essentially motivates the work carried out herein.

More precisely, the active sonar systems are then divided into two distinct configurations according to the location of the transmitter and the receiver [2]. The configuration is said to be monostatic when these two components are colocated and bistatic when they are delocalized.

By extension, a Multistatic Sonar Network (MSN) is then a set of sonar systems in monostatic and/or bistatic configuration.

In addition, in this paper, we focus on a specific category of sonars which are known as sonobuoys[1]. These are consumable acoustic buoys (i.e. with a limited life span) dropped onto the area from an airborne carrier such as a maritime patrol aircraft, a helicopter or an Unmanned Aerial Vehicle (UAV). The sonobuoys are bundled in cylinder-shaped containers and unfold upon impact with the sea surface, prior to submergence to a pre-determined depth from a discrete range of options. See Figure 1 for a simplified illustration of the operational context. These buoys are further subdivided into three broad categories. They can be either transmitters-only, receivers-

[1] Portmanteau formed by "sono" and "buoy"

only or transmitter-receivers and are abbreviated Tx, Rx and TxRx respectively. In each of these three categories, we then find several types of buoys with different performances and intrinsic characteristics (e.g. emission frequency, lifetime, emission power, immersion depths etc.).

In this work, we seek to optimize the spatial configuration of the MSN formed by the various sonobuoys so as to maximize the area covered over a given Area of Interest (AoI). This is done with a prospect of surveillance or target search in a given perimeter (with or without a priori on the position of the target).

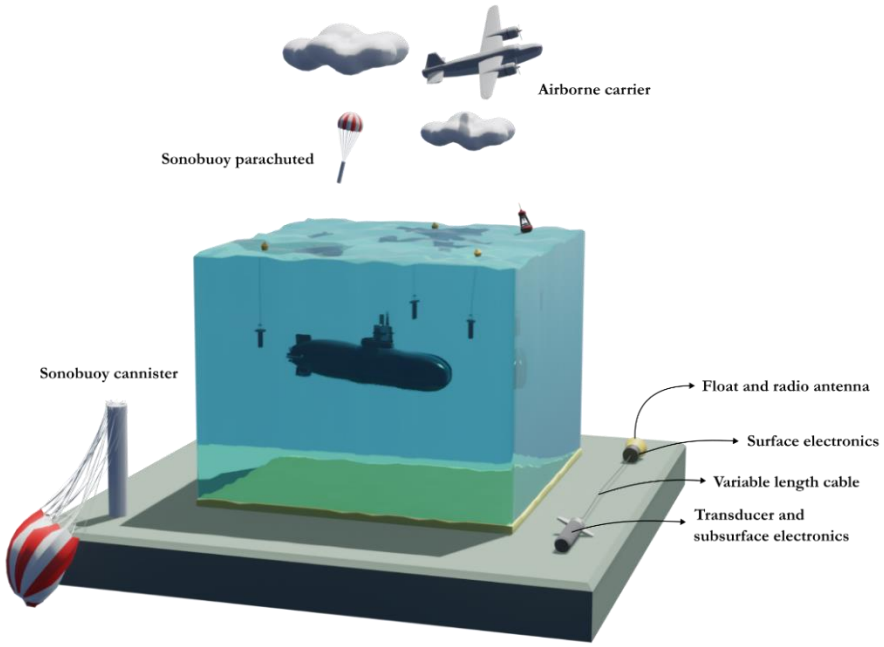

Figure 1: Simplified illustration of the operational context

In the published literature, the buoy placement problem (Tx, Rx, TxRx) has, to the best of our knowledge, never been directly addressed. Indeed, a simplification is regularly made and consists in considering only sources and receivers. Similarly, no work has been done on the heterogeneous case with sensors of different types which brings its own set of issues, notably due to variability between the performances of the different sonar systems and possible inter-sensor incompatibilities (e.g. between a high-frequency sensor and a low-frequency sensor). Last but not least, the case with coastlines has never been explicitly addressed either. See [3], [4], [5], [6] for the most recent work on this topic.

2 Methods Proposed

In the work carried out in this paper, the method retained was the simulated annealing [7]. This choice of a single solution method was strongly constrained by the time needed to evaluate a single solution, making the use of population-based methods (e.g. GRASP, genetic algorithm)

obsolete if one wishes to emphasize overall performance.

Two sets of neighborhood operators have been considered: k-swap and k-n-m-shift. The k-swap consists in performing k swaps in parallel (without overlapping) and the k-n-m-shift consists in moving k sensors on a ring whose thickness is m - n. In other words, if n = 2 and m = 4, it is possible to drag a sensor from 2 to 4 units from its initial position.

Moreover, the initial operating temperature has been chosen to have an initial acceptance rate of 50%, the cooling scheme is a geometric one and the reduction factor is adaptive, i.e. it is systematically recalculated according to the remaining computational budget in order to reach a minimum temperature with an acceptance rate of about 1%. This is the naïve version, in the classical sense.

For the improved version, the basic idea was to use reinforcement learning to prioritize the movements with the highest acceptance rate per unit of CPU time. This was done using the multi-armed bandit principle [8] along with a roulette-wheel type selection [9].

Using the knowledge gathered from several executions on different instances, we were able to identify a better strategy than keeping the same neighborhood for the whole execution, as it is the case in the naïve version.

This new strategy consists in starting from the most aggressive neighborhoods and progressively reducing the "scope" of the neighborhood until reaching a very local and almost surgical neighborhood at the end of the execution (in order to minimize the abrupt jumps within the objective function). We thus have a succession of neighborhoods at regular time intervals, following a funnel principle (from the widest to the narrowest).

3 Illustrative Example

A didactic example showing a solution obtained after the execution of the simulated annealing on a given instance is shown in Figure 2 below. More precisely, it is a 75x75 grid with 4282 maritime cells and 1343 terrestrial cells. Concerning the equipment, there are 3 TxRx buoys (type A: 1; type B: 1; type C: 1), 2 Tx buoys (type D: 2) and finally 4 Rx buoys (type E: 4, type F: 0). As for the performance of the various sonar systems that can be obtained by coupling a transmitter and

Tx \ Rx	A_{HF}	B_{HF}	C_{LF}	E_{LF}	F_{LF}
A_{HF}	5	6	x	x	x
B_{HF}	6	7	x	x	x
C_{LF}	x	x	10	4	2
D_{LF}	x	x	12	6	3

Table 1: Performance of sonar systems (in km)

a receiver, these are summarized in Table 1 hereunder (HF stands for high frequency and LF for low frequency). The detection threshold ϕ has been set at 0.95.

Thus, the sub-figure (a) on the left shows the blank rectangular grid, i.e. the digital elevation model with bathymetric and altimetric data from GEBCO [10], whereas the sub-figure (b) shows the heatmap corresponding to the cumulative detection probabilities of the different targets by the entire network. Note that the white level line represents the detection threshold of 0.95 and thus the boundary of the geometric locus where the cumulative detection probability is above this cut-off.

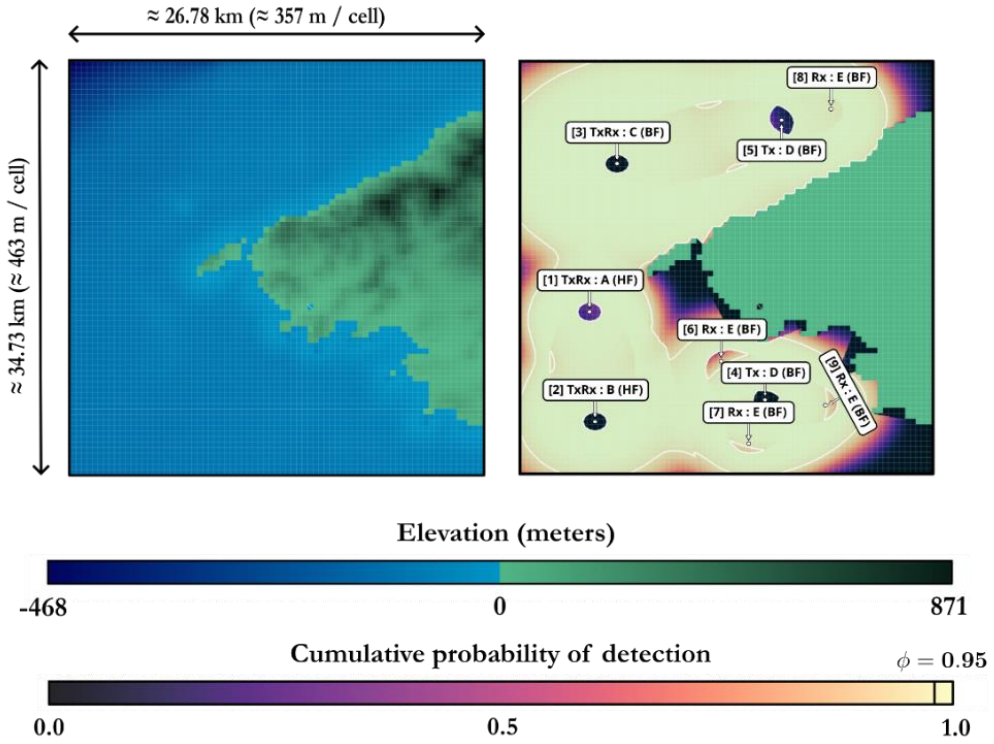

Figure 2: Example of solution

4 Numerical Experiments

For the numerical experiments, the detection threshold and various performances are identical to the ones discussed in the previous section. The Figure 3 below present a sample of experimental results on 2 instances with a thumbnail enabling to glimpse the topology of the targeted instance. Finally, in both cases, 20 resolutions were performed and the computational budget was set at 20 seconds.

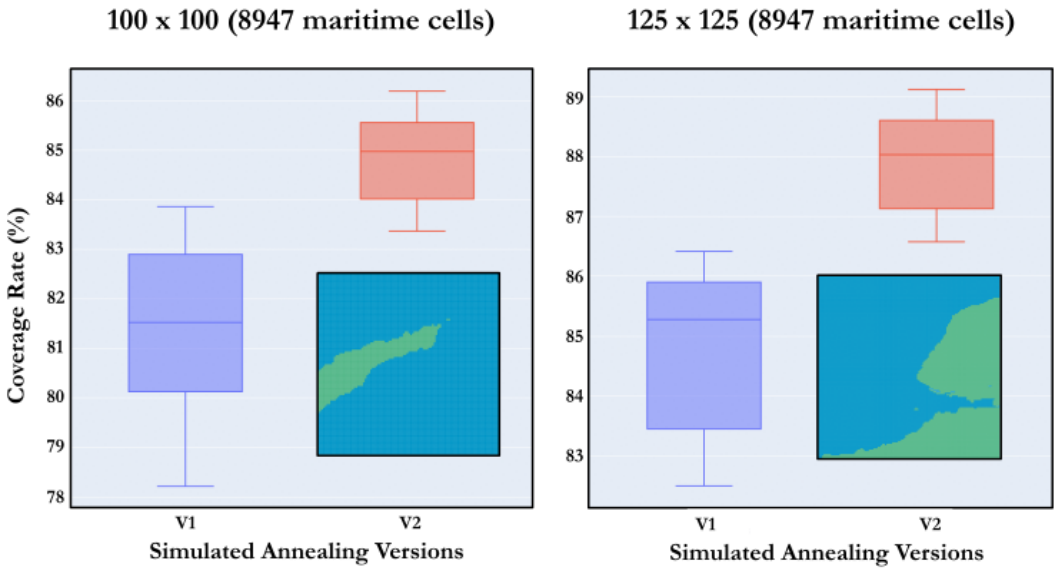

Figure 3: Sample of some experimental results

For the instance on the left, there was 6 TxRx buoys (type A: 2; type B: 2; type C: 2), 4 Tx buoys (type D: 4) and finally 4 Rx buoys (type E: 2, type F: 2). For the instance on the right, there were 5 TxRx buoys (type A: 2; type B: 2; type C: 1), 6 Tx buoys (type D: 6) and finally 8 Rx buoys (type E: 4, type F: 4).

References

[1] Urick, R.J., 1983. Principles of underwater sound. 3rd ed., McGraw-Hill, New York.

[2] Washburn, A.R., 2010. A multistatic sonobuoy theory. Technical Report NPS-OR-10-005. Naval Postgraduate School. Monterey, California.

[3] Fügenschuh, A.R., Craparo, E.M., Karatas, M., Buttrey, S.E., 2020. Solving multistatic sonar location problems with mixed-integer programming. Optimization and Engineering 21, 273–303. doi:10.1007/s11081-019-09445-2.

[4] Craparo, E.M., Karatas, M., 2018. A Method for Placing Sources in Multistatic Sonar Networks.Technical Report NPS-OR-18-001. Naval Postgraduate School. Monterey, California.

[5] Craparo, E.M., Fügenschuh, A., Hof, C., Karatas, M., 2019. Optimizing source and receiver placement in multistatic sonar networks to monitor fixed targets. European Journal of Operational Research 272, 816–831. doi:10.1016/j.ejor.2018.02.006.

[6] Craparo, E.M., Karatas, M., 2020. Optimal source placement for point coverage in

active multistatic sonar networks. Naval Research Logistics 67, 63–74. doi:10.1002/nav.21877.

[7] Rutenbar, R.A., 1989. Simulated annealing algorithms: An overview. IEEE Circuits and Devices magazine 5, 19–26.

[8] Kuleshov, V., Precup, D., 2014. Algorithms for multi-armed bandit problems. Journal of Machine Learning Research.

[9] Lipowski, A., Lipowska, D., 2011. Roulette-wheel selection via stochastic acceptance. Physica A: Statistical Mechanics and its Applications 391. doi:10.1016/j.physa.2011.12.004.

[10] GEBCO Bathymetric Compilation Group, 2022. The GEBCO 2022 grid - a continuous terrain model of the global oceans and land. doi:10.5285/e0f0bb80-ab44-2739-e053-6c86abc0289c.